Tungsten-series impurity diffusion in single-crystal tungsten

N. K. Arkhipova, S. M. Klotsman, I. P. Polikarpova, G. N. Tatarinova, A. N. Timofeev, and L. M. Veretennikov
Institute of Metal Physics, Ural Science Research Centre of the U.S.S.R. Academy of Sciences, Sverdlovsk, U.S.S.R.
(Received 5 March 1984)

The temperature dependences of the volume-diffusion coefficients of Ta, Re, Os, Ir, and W have been measured for tungsten single crystals by the sectioning method. The analysis of our data and results obtained by other authors shows that the Arrhenius dependence of self-diffusion coefficients possesses no curvature. The physically lucid and simple Lazarus—Le Claire model for the vacancy mechanism semiquantitatively describes our experimental $Q(z)$ dependences for impurities (standing on the right-hand side of W) in the tungsten series. For Ta the activation energy Q is less than or equal to the Q for self-diffusion. This behavior is very similar to what is observed for the diffusion of Co in Ni. This indicates that either little or no positive excess charge is localized on the Ta impurity in W.

I. INTRODUCTION

Exact impurity-diffusion-parameter measurements for crystals are one of the sources of information for (a) the mechanism of impurity diffusion, (b) the nature of the interaction of an impurity with point defects participating in an elementary diffusion event, and (c) some characteristics of the state of an impurity in a crystal.

The impurity-diffusion-vacancy mechanism model of metals, created by Lazarus[1] and developed by Le Claire[2,3] (hereafter referred to as the LLC model), has become a major tool in interpreting the results of diffusion studies and has established a diffusion experiment performance level indispensable for extracting physical information from impurity-diffusion parameters.

The LLC model is based on three simple assumptions.

(1) The impurities from the same Periodic Table series as the solvent may be described as an excess impurity-site point charge Z_2e screened by conduction electrons. The magnitude of this charge for nontransition solvents and impurities is determined as the difference of their valences.

(2) The other point defect participating in an elementary diffusion event, i.e., the vacancy, may be treated similarly. Its charge excess $-Z_1e$ is equal in magnitude to the valency of the solvent element, but opposite in sign.

(3) The Coulomb interaction of the screened excess charges of these two point defects, at all stages of the elementary diffusion event, determines the difference in the enthalpies of activation for impurity diffusion and self-diffusion.

In terms of this model, the difference in the enthalpies of activation for impurity diffusion and self-diffusion, ΔQ, is

$$\Delta Q = -\frac{\alpha Z_1 Z_2 e^2}{r}\exp(-qr) - C \ , \tag{1}$$

where α is a constant dependent on Z_2 only, r is a coordinate, q is a screening constant, and C is a correlation correction.

Attempts to describe the diffusion of impurities with a positive excess charge in nontransition solvents[4] (aluminum, copper, silver, gold, and zinc) have shown that this model possesses high predictive power and that the diffusion experiment's resolution is sufficiently high to permit derivation of physical information. The LLC model gives an equally good fit to the diffusion parameters of simple and transition impurities having a negative excess charge.[5,6]

It was therefore natural to test the applicability of this physically lucid and attractive model for describing the diffusion in transition-element crystals. It was indicated in every way that the diffusion of simple impurities in solvents such as nickel would be describable in terms of the LLC model.

The results of systematic research on diffusion in nickel[7] have demonstrated that experimental results and LLC model calculations are in excellent quantitative agreement. In analyzing the impurity-diffusion results for nickel, the use of the magnetic properties of the corresponding highly dilute solid solutions in determining the excess charges of the impurities in nickel was found to be highly essential.

It would seem that the LLC model approximations would be too crude for crystals of the elements located in the middle of the long transition periods and that the diffusion of impurities (arranged in the same Periodic Table series with the solvent) differing from the solvent only in excess charge could not be described by relation (1). It is known, however, that in the free-electron approximation the lattice oscillations in these metals are described better than those in nontransition-element crystals.[8] This led us to believe that the LLC model would also be able to describe regularities of the diffusion in systems based on crystals of the elements which are in the middle of the large periods of the Periodic Table.

II. EXPERIMENTAL TECHNIQUES

The diffusion coefficient D was measured using the radiometric diffusion zone-sectioning method. Diffusion from an "instantaneous" source into a "semi-infinite"

specimen was performed. For these initial boundary conditions, the concentration distribution in the diffusion zone is given by

$$C(x,t)=\frac{S}{(\pi Dt)^{1/2}}\exp(-x^2/4Dt)\ . \quad (2)$$

Here $C(x,t)$ is the concentration distribution of the tracer along the diffusion direction x, t is the diffusion annealing time, and S is the amount of tracer in the source for $t=0$.

A. Materials and specimen preparation

Tungsten single crystals 6—9 mm in diameter were grown at the Institute of Metal Physics (Ural Science Research Centre of the USSR Academy of Sciences) by the method of electron-beam crucibleless zone melting in vacuum[9] (10^{-5} Pa). The dislocation density of single crystals was 10^4—10^5 cm^{-2}, the initial ratio of the residual resistivities δ at 300 and 4.2 K being $\delta=\rho_{300}/\rho_{4.2}=2\times10^4$—$5\times10^4$.

The single crystals were cut into (3—4)-mm-thick discs by the electric spark method. Subsequent to cutting, the distorted surface layer (total thickness of about 500×10^{-4} cm) was successively removed by grinding (about 50×10^{-4} cm), electropolishing (about 350×10^{-4} cm), and anodic oxidation [about $(3-5)\times10^{-4}$ cm]. X-ray topography was employed to check whether the distorted layer was completely removed. The structure of the Laue pattern spots from the flat surfaces thus prepared did not differ from that of the spots obtained from the initial single crystal.

For the diffusion source the radioactive isotopes ^{187}W, ^{182}Ta, ^{186}Os, and ^{192}Ir were used. These isotopes were produced by neutron irradiation of pure (99.99—99.9999 %) metals or stable isotopes (rhenium as an enriched mixture: 95 at. % ^{185}Re and 5 at. % ^{187}Re).

The diffusion source was created by electron-beam evaporation. The high specific activity of the metals irradiated (4—10 Ci/g) ensured the instantaneous-source conditions by evaporating sufficiently thin tracer layers and assured high activity in the diffusion zone.

B. Diffusion annealing

The diffusion specimens were introduced into tubular capped tungsten containers preliminarily cleaned by electropolishing and annealed at temperatures exceeding the possible diffusion-annealing temperatures. The specimen-filled containers were placed into a massive tungsten "black-body" model shell [(0.5—1)-cm-thick walls], serving at the same time to level out furnace temperature gradients. Prior to the time of the diffusion experiments, the shell had been annealed. The quality of the shell as a black-body model was tested with reference to the platinum and iridium melting points which were (1775±8) °C and (2448±6) °C, respectively. The diffusion annealing was carried out in a 10^{-3}—10^{-4} Pa vacuum in a resistive heating furnace over the temperature range between 1730 and 2690 °C. The annealing temperature was maintained constant to within ±2° by an automatic temperature controller. The junction of the controlling W-Re thermocouple was fastened onto one of the resistive-heater screens.

The annealing temperature was determined by means of a disappearing-filament-reference pyrometer. The temperature was recorded by a multipurpose photoelectric pyrometer. Corrections were introduced for the absorption of black-body radiation in the furnace sight glasses and in the total internal reflection prism employed to deflect the light flux to a horizontal plane. To determine these corrections after each diffusion annealing, the absorption of the radiation of a reference tungsten strip lamp in the sight glasses and prism over a (1500—2000)-°C temperature interval was measured. The true diffusion-annealing temperature was calculated by interpolating or extrapolating these dependences. With respect to the uncertainty of these corrections, the error of the annealing temperature was 5—10 °C for the temperature range from 2200 to 2700 °C and from 1 to 3 °C for the range from 1800 to 2200 °C.

Specimen heating and cooling time corrections were introduced from continuous black-body temperature records by an automatic pyrometer.

C. Sectioning

The diffusion zones of 0.3×10^{-4}—3×10^{-4} cm were divided into layers by the anodic oxidation method.[10] Anodic oxidation was carried out in a solution of 40 g/l of KNO_3+2 ml of HNO_3 at 20 to 70 V. The oxide film was removed in an alkaline solution of 3 g of KOH per liter of H_2O. The thickness d of the removed layers was determined by the voltage V across the anodic bath from the experimental calibration curve. The latter was plotted from results of straightforward weight measurements of the thickness of the layer which was removed by anodic oxidation of a tubular tungsten single crystal about 20 cm^2 in surface area.

A check was made on the possibility of using the $d(V)$ curve, obtained on pure tungsten and used to determine the thickness of removed layers in self-diffusion experiments, to determine the thickness of removed sections in impurity-diffusion zones. To this end, iridium- and tantalum-diffusion zones were produced on tubular tungsten single crystals. The thickness of the layers removed by anodic oxidation was determined by straightforward weight measurements for several values of V. The values of the thicknesses of the removed layers in the impurity diffusion zone, determined by weight, coincided with the values from the $d(V)$ curve for pure tungsten to within ±5% [the accuracy of the determination of the layer thickness from the $d(V)$ curve]. In all subsequent impurity-diffusion measurements we therefore used the earlier measured $d(V)$ dependence for pure tungsten.

However, when anodizing impurity-diffusion zones, difficulties were encountered which were absent in the case of self-diffusion. A substantial portion of the impurity tracer emerged in the electrolyte. Therefore, to correctly measure the activity of the removed layer, it was necessary to collect not only the alkaline solution in which the oxide was dissolved, but also the acid bath.

In addition, a check was made on the possible accumulation of the impurity tracer on the tungsten under the ox-

ide film due to the impurity being "driven away" during the formation of an oxide layer. To prove this, we measured the integral residual radiation intensity, and the $z(x)$ dependences were analyzed, where $z = x/(2\sqrt{Dt})$.

With z varying up to 2 or 3 (diffusion zone depths of up to 7×10^{-4} cm with layer thickness of up to 0.1×10^{-4} cm) the experimental points fell satisfactorily on the straight line $z(x)$, the slope of this line giving the same D value as that given by the straight line $C(x)$ obtained from removed-layer activity measurements.

For diffusion zones larger than 3×10^{-4} cm layers of about 0.5×10^{-4} cm thickness and more were removed by grinding. The layer thickness was determined from the difference of the weights of the specimen before and after layer removal and from the specimen diameter. After the diffusion anneal, the specimen was electric-spark-machined into the correct cylindrical shape, which also simultaneously eliminated possible radioactive contamination of the lateral sides. The layer thickness determination error did not exceed 1—2 %.

Comparison of both layer-removal methods was performed on specially selected diffusion zones. The results obtained using the two methods were shown to coincide completely.

Radioactive sections were measured with the use of a single-channel analyzer having a well-type scintillation detector into which calibrated fluoroplastic vials were placed. The tracer gamma-peak intensities were measured. All the necessary corrections were introduced by measuring standard samples made of the same preparations which were used as tracers. The radioactive section measurement error did not exceed 1%.

D. Diffusion zone purity check

It was shown in preliminary experiments on self-diffusion in tungsten that the value of the measured diffusion coefficient depends largely on the initial purity of the tungsten single crystals used. The diffusion coefficients measured on less pure (according to the supplier's certification) crystals turned out to be higher than those measured on purer crystals, particularly in the low-temperature region.

However, even in the cases when high-purity ($\delta > 10^3$) crystals were employed, one could not be sure that there occurred no contamination of the diffusion zone during diffusion annealing. Only inspecting the purity of the diffusion zone could, therefore, enable us to obtain or to select correct results. For these reasons we used the non-contact eddy-current method of measuring the residual resistivity[11] of the specimens before and after sectioning.

Simulation annealing of reference specimens (without a diffusion source) led to a decrease of δ from 10^5—10^4 in the initial specimens to 10^4—10^3. The use of a carrier-free cyclotron tracer ^{181}W (in the form of an aqueous solution of $NaWO_4$ evaporated on the working surface of the diffusion specimen) as the diffusion source resulted in an appreciable contamination of the diffusion zone. In such diffusion zones [the effective penetration $(Dt)^{1/2} \simeq 10^{-5}$ cm] the quantity δ decreased to a level of 10^2, which corresponded to 99.9% purity.

When investigating the impurity diffusion in tungsten, the values measured subsequent to diffusion annealing could not be used to characterize the purity of the diffusion zone. Therefore, reliable measures were taken to maintain the purity of tungsten crystals during diffusion annealing at a level of $\delta \geq 10^4$.

E. Checking the uniformity of tracer distribution in the diffusion zone

When prepared for diffusion annealing, as described in the previous sections, the specimens were subjected to intensive mechanical working: electric spark machining, grinding, and polishing. Therefore, despite the measures taken to remove distorted surface layers, the possibility existed that the zone adjacent to the working surface was not free from cracks. Apart from this, the use of intensive electropolishing to remove thick layers upon mechanical polishing led to the occurrence of a relief whose depth might prove to be comparable with $(Dt)^{1/2}$. In order to detect defects that would be capable of altering, particularly at lower diffusion-annealing temperatures, the diffusion zone concentration distribution measured, the uniformity of the diffusing element distribution at various diffusion zone depths was checked by autoradiography.

It was shown that in all the cases when the penetration plots had "tails" or a continuous curvature (the latter, as a rule, at temperatures below 1750 °C) the autoradiograms displayed a nonuniform tracer distribution: Against a weak background, the loci of preferential tracer localization were revealed.

Since it had not been possible to ascertain the correlation between the prominence of these anomalies with the diffusion-annealing temperature or time even when the same specimen was used, the conclusion was drawn that the observed failures of Eq. (2) are not due to diffusion through defects such as dislocations or subgrain boundaries. Those results were just not used.

III. RESULTS

The penetration plots for self-diffusion in tungsten for all the temperatures investigated are good straight lines when the concentration varies by 2—3 orders of magnitude.[12] However, at temperatures below 2000 K it has not been possible to obtain a diffusion zone concentration distribution corresponding to Eq. (2): The linear part could be singled out on none of the segments.

Figure 1 presents typical penetration plots for the diffusion of tantalum in tungsten. Penetration plots for the diffusion of rhenium in tungsten are given in Ref. 13. Here, the lower boundary of the temperature range in which we have obtained good straight lines, $\ln C(x^2)$, has risen to 2100 K. For temperatures between 2100 and 2900 K we have obtained linear penetration plots for tantalum concentrations varying by 2—3 orders of magnitude.

The depth profiles for the diffusion of osmium and irridium are given in Figs. 2 and 3, respectively. For iridium as well as for the other impurities investigated, the lower limit of the temperature interval where no "tails" manifest themselves lies in the vicinity of 2100 K, whereas for

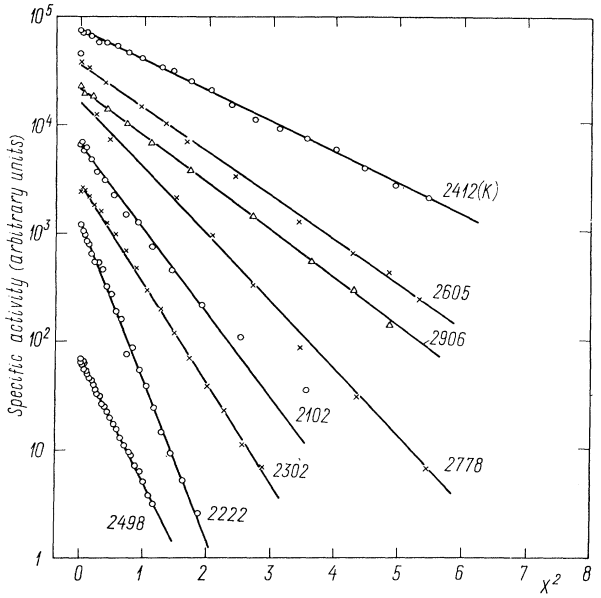

FIG. 1. Typical penetration plots for ^{182}Ta diffusion in W. Each division on the abscissa represents: 10^{-6} cm^2 for the 2906-, 2778-, and 2605-K curves; 10^{-7} cm^2 for the 2498-K curves; 10^{-8} cm^2 for the 2412-, 2302-, and 2222-K curves; 10^{-9} cm^2 for the 2102-K curve.

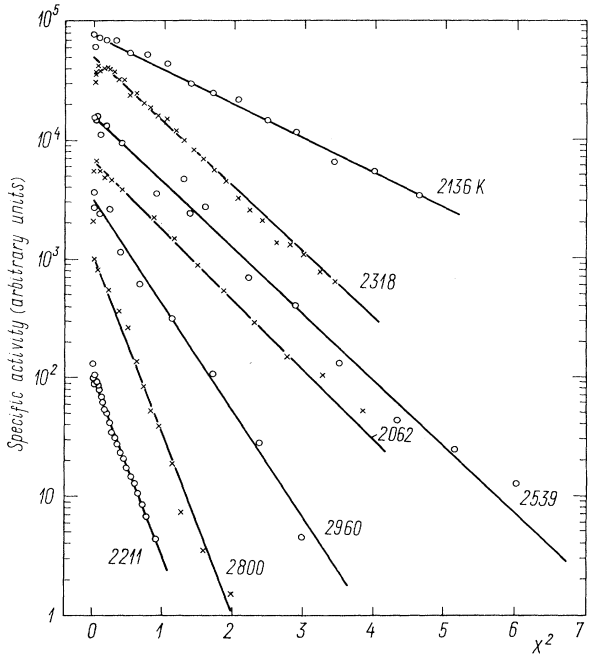

FIG. 3. Typical penetration plots for ^{192}Ir diffusion in W. Each division on the abscissa represents 10^{-5} cm^2 for the 2960- and 2800-K curves; 10^{-6} cm^2 for the 2539-K curves; 10^{-7} cm^2 for the 2318- and 2211-K curves; 10^{-8} cm^2 for the 2136- and 2062-K curves.

osmium it rises to 2200 K.

Over the temperature interval investigated the diffusion coefficients vary by 4 orders of magnitude from 10^{-10} cm^2/s (see Tables I—III and Fig. 4). Rather than resort to the conventional presentation of experimental values in a $\ln D$—$(1/T)$ plot to specify the temperature dependences of the diffusion coefficients, we use deviation plots which are shown in Fig. 5. The relative deviations of the measured diffusion coefficient values from the calculated curve, obtained using the least-squares method, are plotted versus the diffusion-annealing temperatures. This representation enables us to describe more clearly the quality of the temperature dependence of the diffusion coefficients: We can see the presence or absence of systematic deviations of the measured values from the temperature dependence of the diffusion coefficients which has been adopted in the calculation of the model, etc.

As can be seen, the coefficients measured for the self-diffusion and diffusion of rhenium in tungsten lie in a ±20% band. In the other cases the band is about ±10%. The temperature-dependence parameters for the diffusion coefficients are presented in Table IV.

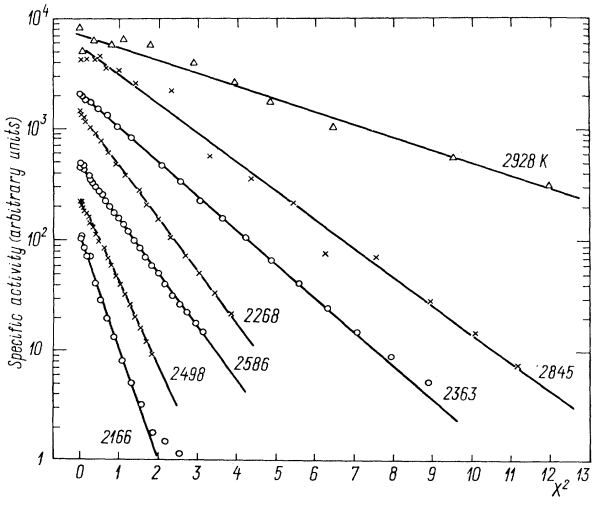

FIG. 2. Typical penetration plots for ^{191}Os diffusion in W. Each division on the abscissa represents 10^{-6} cm^2 for the 2928- and 2845-K curves; 10^{-7} cm^2 for the 2586- and 2498-K curves; 10^{-8} cm^2 for the 2363-, 2268-, and 2166-K curves.

IV. DISCUSSION

A. Self-diffusion in tungsten

To analyze the results on the self-diffusion in tungsten, let us examine the deviation plots (Fig. 6) of the diffusion

TABLE I. Diffusion of tantalum in tungsten.

Temperature (K)	Annealing time (s)	D (cm^2 s^{-1})
2906[a]	2.773×10^3	8.839×10^{-11}
2778[a]	5.144×10^3	3.273×10^{-11}
2605[a]	4.591×10^4	5.672×10^{-12}
2498	6.337×10^3	1.529×10^{-12}
2412	6.090×10^3	6.173×10^{-13}
2302	7.951×10^3	1.442×10^{-13}
2222	1.578×10^4	4.743×10^{-14}
2102	1.688×10^4	6.640×10^{-15}

[a]Sectioning by grinding.

TABLE II. Diffusion of osmium in tungsten.

Temperature (K)	Annealing times (s)	D ($cm^2 s^1$)
2928[a]	5.220×10^3	1.774×10^{-10}
2845[a]	4.842×10^3	8.620×10^{-11}
2586	2.704×10^3	7.943×10^{-12}
2498	4.137×10^3	3.406×10^{-12}
2363	4.494×10^3	7.802×10^{-13}
2355	4.254×10^3	7.652×10^{-13}
2296	2.429×10^4	3.728×10^{-13}
2302	2.340×10^3	3.710×10^{-13}
2268	8.526×10^3	2.634×10^{-13}
2220	8.616×10^3	1.313×10^{-13}
2166	1.282×10^4	7.769×10^{-14}
2105	1.728×10^4	2.894×10^{-14}

[a]Sectioning by grinding.

coefficients measured by us and in Refs. 14 and 15. As is evident from Fig. 6(a), our results and the data obtained in Ref. 14 give a good fit to the general ln$D$-versus $1/T$ dependence with the parameters specified in Table V. Mention should be made of the relatively small spread of the measured D values: the mean deviation $\Delta D/D = \pm 12.5\%$. As correctly noted by the authors of Ref. 15, it is not difficult in a relatively narrow temperature interval to obtain an Arrhenius plot of volume-diffusion coefficients with a relatively small statistical spread of experimental points.

Now let us discuss the results of Ref. 15 in which the self-diffusion in tungsten was measured over a wide temperature range from 1700 to 3400 K. Primarily, it will be observed that at the lowest temperatures of the interval investigated, viz., at 1791 to 1705 K, the quantity $(Dt)^{1/2}$ is $(2-7)\times10^{-7}$ cm and the total diffusion zone depth analyzed is of the order of 2×10^{-6} cm. Under these conditions, the preparation quality of the working surface of the specimens to be investigated acquires particular importance. The presence on the surface of a relief comparable in depth with $(Dt)^{1/2}$ as well as the high density of dislocations persisting due to the previous mechanical preparation, may fatally affect the concentration distribution measured in so narrow a diffusion zone.

Since Ref. 15 contains no indication as to what steps were taken in inspecting the quality of the surface and of

TABLE III. Diffusion of iridium in tungsten.

Temperature (K)	Annealing times (s)	D ($cm^2 s^{-1}$)
2960[a]	4.088×10^3	3.236×10^{-10}
2906	2.784×10^3	2.721×10^{-10}
2800[a]	5.201×10^3	1.229×10^{-10}
2539[a]	1.464×10^4	1.266×10^{-11}
2318	1.336×10^4	1.417×10^{-12}
2267	2.087×10^4	7.534×10^{-13}
2211	1.862×10^4	3.729×10^{-13}
2136	2.670×10^4	1.377×10^{-13}
2080	2.192×10^4	5.511×10^{-14}
2062	3.866×10^4	4.826×10^{-14}
2007	1.953×10^4	2.207×10^{-14}

[a]Sectioning by grinding.

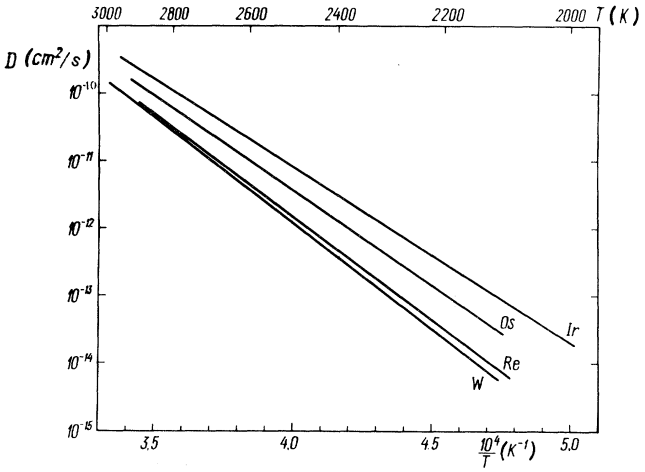

FIG. 4. Temperature dependences of volume-diffusion coefficients of Ta, Re, Os, Ir, and W in single-crystal tungsten.

the crystal zone adjacent to it, we consider it possible to exclude from our consideration the D values measured from 1791 to 1705 K. The other values are given in Fig. 6(b) as deviations of the experimental values from the single Arrhenius dependence.

As can be seen, the mean deviation of the diffusion coefficients amounts to around 42%, which is much higher than that in Fig. 6(a). However, a considerable contribution to this quantity is made by the unit points which deviate by 100—300 %. As noted in Ref. 15, when removing layers by anodic oxidation a mask restricting the area of analysis was used on the working surface of the specimen. The contingency that the lateral sides of

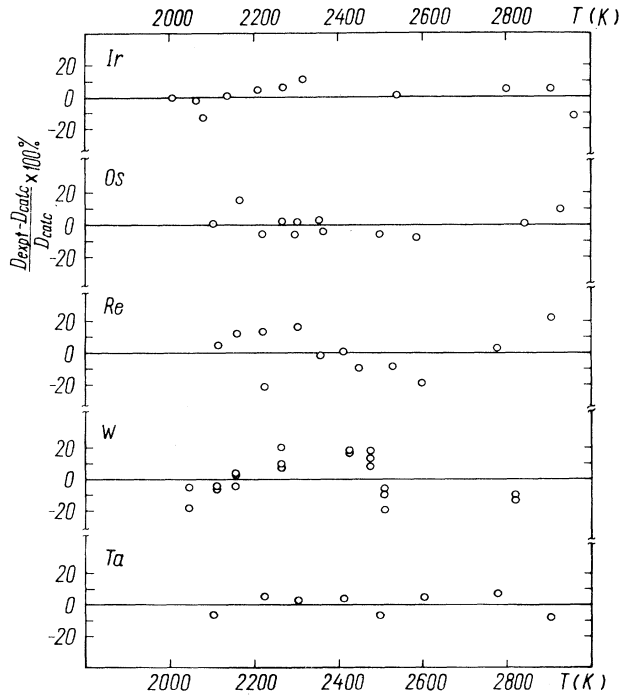

FIG. 5. Deviation of D_{expt} for impurity and self-diffusion in tungsten from the calculated straight lines.

TABLE IV. Temperature-dependence parameters for the diffusion coefficients.

Tracer	Temperature interval (K)	D_0 ($cm^2 s^{-1}$)	Q (kcal mol^{-1})	ΔQ_{expt}	ΔQ_{calc}
^{182}Ta	2020—2900	$6.2\ ^{+1.6}_{-1.3}$	143.7±1.2	−5.9	
^{187}W	2040—2820	$15.3\ ^{+5.7}_{-4.2}$	149.6±1.4		
^{186}Re	2110—2900	$4.0\ ^{+2.1}_{-1.4}$	142.6±2.0	−7.0	−7.7
^{191}Os	2100—2930	$0.64\ ^{+0.16}_{-0.12}$	128.6±1.4	−21.0	−15.4
^{192}Ir	2000—2960	$0.32\ ^{+0.07}_{-0.06}$	120.9±0.9	−28.7	−20.2

the crater that formed might be etched was not dismissed. Thus, there could obviously arise concentration profiles yielding diffusion coefficients that are too large. These strongly deviating points substantially perturb the balance of positive and negative deviations. For these reasons and from formal considerations (the deviations exceed 2σ) the results with ±100—300% deviations will not be considered henceforth.

The remaining set of experimental self-diffusion coefficient values from Ref. 15 lies in a ±25% band. Formally, taking account of this spread, there are no grounds for revealing systematic deviations of the experimental values from the $\ln D$—$(1/T)$ plot. However, let us consider the situation depicted in Fig. 6(b). The positive and negative deviations are seen to be mutually compensated in the intervals of 1800—2200 K, 2600—2800 K, and 3000—3200 K. And it is only in the (2200—2400)-K and (2800—3000)-K intervals that the negative deviations prevail, the positive deviations dominating in the (3200—3400)-K interval. Since the intervals with the same sign of deviations from the Arrhenius dependence have a sufficiently random distribution over the entire temperature range studied, there is every indication that the use of a single exponent to describe the self-diffusion in tungsten is a good approximation.

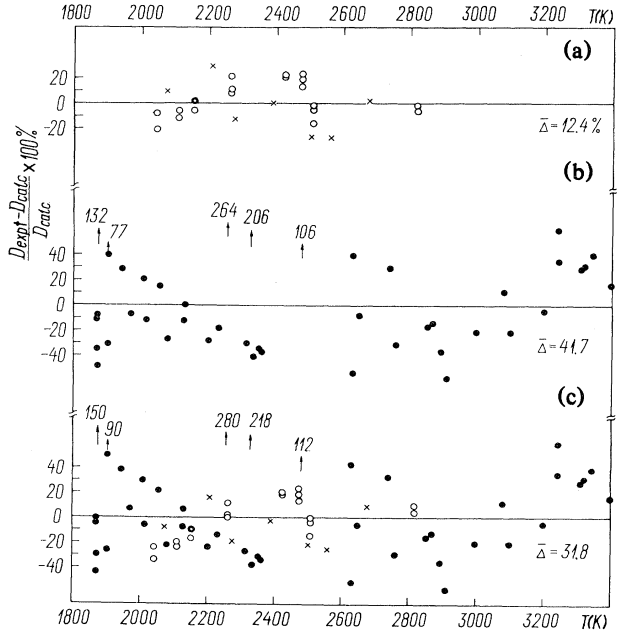

FIG. 6. Deviation of D_{expt} for self-diffusion in tungsten from the calculated straight line: ○, Ref. 12; ×, Ref. 14; ●, Ref. 15.

This impression strengthens if one considers conjointly the most reliable measurements of the self-diffusion coefficients in tungsten [Fig. 6(c)]. As can be seen, the results obtained in this paper and in Ref. 14 completely overlap those of Ref. 15 and almost entirely eliminate the asymmetry of the deviations in the (2200—2600)-K interval. It is evident to us that the data presented in Fig. 6(c) demonstrate the absence of significant deviations of the self-diffusion coefficients in tungsten from single exponential behavior, the parameters of which are given in Table V. In our view, these parameters are the most correct at present.

The conclusion of the Arrhenius dependence of the coefficients of self-diffusion in tungsten over a wide temperature range from 1800 to 3400 K [$(0.49—0.92)T_m$] is in good agreement with the result of Refs. 16 and 17, where it has not been possible to detect the curvature of the Arrhenius dependence of the self-diffusion coefficients in chromium in the temperature interval (1073—2090)-K [$(0.51—0.99)T_m$]. Hence it may be considered that the result of Ref. 18 in which the curvature of the Arrhenius dependence of the self-diffusion coefficients in molybdenum was detected is an exception and needs to be reproduced. This reproduction is all the more necessary because the sectioning aimed at measuring the self-diffusion coefficients in molybdenum at low temperatures (below $0.76T_m = 2200$ K) was done involving the use of ion sputtering.[18] In this case a crater formed on the diaphragm-restricted area of the specimen. Sputtered jointly with the specimen, the diaphragm becomes larger in diameter. As a result, the material sputtered is redistributed within the crater, etc.[19] and there arises the danger of the crater-wall activity emerging in the less active, deeper layers. This is a standard situation which one con-

TABLE V. Parameters for the self-diffusion coefficients in tungsten.

	D_0 ($cm^2 s^{-1}$)	Q (kcal mol^{-1})	$\Delta D/D$ (%)	Ref.
W→W	$10^{+4.0}_{-2.9}$	147.7±1.6	12.4	12,14
W→W Temperature range 1869–3409 K	$3.7^{+1.7}_{-1.2}$	142.7±1.7	41.7	15
W→W Excluding points with $\Delta > 2\sigma$	$5.5^{+1.5}_{-1.2}$	145.0±1.1	24.9	15
W→W Combined calculation of selected data	$6.0^{+1.2}_{-1.0}$	145.3±0.8	20.3	12,14,15
Cr→Cr	1280 ± 230	105.6±0.7		16,17

fronts when analyzing diffusion profiles by the secondary-ion mass spectrometry technique (SIMS). In order to use sputtering as a method of sectioning diffusion zones with radioactive tracers, it is apparently necessary to employ at least the technique already optimized in SIMS: collecting, for measurements, the material sputtered only from the central crater portion which is sufficiently far from the edges. Perhaps gradually decreasing the diameter of the diaphragm, which limits the cross section of the beam, as layers are sputtered may assure a still more reliable suppression of the crater-wall effect. Whether or not the crater effect is suppressed completely may be checked by analyzing the radioactive-tracer distribution in a specimen with a thin tracer layer of known thickness lying at different depths, as was done in Ref. 20.

The tungsten and chromium self-diffusion parameters presented in Table V are in excellent agreement with the empirical regularities of the variations of activation energies and preexponential factors for crystals of the transition metals situated in the middle of the Periodic Table.[21]

B. Impurity diffusion in tungsten

As stated in the Introduction, the choice of the impurities investigated was initiated by the desire to test the applicability of the Lazarus–Le Claire concept to crystals of the elements arranged in the middle of the large transition series of the Periodic Table. As in the investigation of the systems on which these concepts had worked very well, we assumed that the impurities standing on the right of solvent tungsten possessed a positive excess charge $Z_2 e$ and that those standing on the left of it possessed a negative excess charge with respect to the solvent. It was therefore expected that tantalum would be a slowly diffus-

TABLE VI. Impurity diffusion in copper.

Impurity	Z	D_0 ($cm^2 s^{-1}$)	Q (kcal mol^{-1})	ΔQ (kcal mol^{-1})	Ref.
Fe		1.40	51.80	−1.30	24
	−3	1.36	52.00±1.2	−1.50±1.2	25
		1.01 ± 0.23	50.95±0.46	−0.45±0.7	26
Co	−2	0.28	54.10	−3.60	26
		1.93	54.10	−3.60	24
Ni	−1	3.8 ± 0.2	56.80±0.10	−6.30	27
		2.7	56.50	−6.0	24
Rh	−2	$3.3^{+0.9}_{-0.7}$	58.0 ±0.6	−7.5 ±0.8	28
Pd	−1	$1.71^{+0.23}_{-0.21}$	54.4±0.3	−3.9 ±0.5	29
Ir	−2	$10.6^{+11.8}_{-5.6}$	66.0 ±1.8	−15.5 ±2.0	6
Pt	−1	$0.67^{+0.26}_{-0.19}$	55.70±0.78	−5.2 ±1.0	30

ing impurity, whereas rhenium, osmium, and iridium would be rapidly diffusing ones. Table IV presents parameters for the temperature dependences of the diffusion coefficients for the systems investigated. In this table values of Q and D_0 for the self-diffusion are taken from our work[12] (see Fig. 5). To calculate the differences in the enthalpies of activation for self-diffusion and heterodiffusion in terms of the LLC model,[2,3] we have used the following values of the parameters. The screening constant q was calculated in terms of the free-electron model according to the formula

$$q_W^2 = q_{Ag}^2 \gamma_W / \gamma_{Ag} , \quad (3)$$

where $q_{Ag}=1.70$ Å^{-1} from Ref. 2; $\gamma_{Ag}=0.646$ mJ/mol deg^2; $\gamma_W=1.30$ mJ/mol deg^2.[22] The parameter α has been calculated from the data of Ref. 23.

For positive Z_2e impurities, as seen from Table IV and Fig. 7, the major conclusions of the LLC model hold qualitatively: With increasing positive excess charge in the tungsten, rhenium, osmium, and iridium series, the activation energy decreases practically linearly. Comparison of the experimental and theoretical values for ΔQ (Table IV) shows that the LLC model gives a semiquantitative description of the diffusion in systems whose properties, even to a crude approximation, hardly satisfy the major premises of this approach: point localization of excess charge on point defects responsible for diffusion (impurity ion and vacancy), the Thomas-Fermi potential of the interaction of these point defects, the free-electron approximation for carriers in the solvent, etc.

As is seen from Table IV and Fig. 4, the diffusion coefficients of tantalum as well as the other impurities investigated are higher than the self-diffusion coefficients and $\Delta Q(\mathrm{Ta})<0$. From the latter it follows, if we exclude from consideration the possibility of incorrect diffusion measurements, that tantalum in tungsten possesses a positive charge excess. But if we take the best value $Q_{self}=145.3$ kcal/mol (see Table V), then within 2σ the Q for tantalum and tungsten coincides. Consequently $Z_2e(\mathrm{Ta})\geq 0$.

A similar situation apparently also occurs for the impurity diffusion in nickel, which is representative of the metals placed at the beginning and at the end of the large transition series of the Periodic Table. Thus the enthalpy of activation of cobalt diffusion in nickel[31] is exactly equal to the Q of self-diffusion (67.6±0.1) kcal/mol, while the diffusion coefficients of cobalt are higher than those of nickel because of $(D_0)_{Co}>(D_0)_{Ni}$.

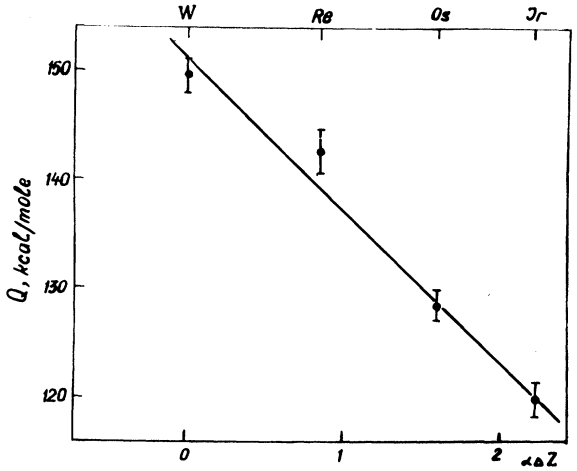

FIG. 7. Dependence of experimental values of activation energy Q_{expt} on excess charge of tracer.

This situation for solvents with incomplete d shells differs qualitatively from the regularities of the diffusion of "electronegative" impurities in copper. It is shown in Refs. 6 and 24–30 that, as the excessive negative charge of the impurities in copper increases, the enthalpy of activation of diffusion rises (Table VI).

V. CONCLUSIONS

It has been shown that the physically lucid and simple LLC vacancy-mechanism model of diffusion is applicable also to the diffusion of impurities (Ta, Re, Os, Ir) standing in the same row of the Periodic Table with the solvent W (crystal of an element arranged in the middle of the large transition period). Analysis of our own data and of the results obtained by other authors permits the conclusion that the Arrhenius dependence of self-diffusion coefficients possesses no curvature. For positive-excess-charge impurities standing on the right in the tungsten series, the LLC model semiquantitatively describes the experimental $\Delta Q(Z_2)$ dependence. Just as for the case of Co diffusion in Ni,[31] only little or no positive excess charge is localized on the Ta impurity in tungsten. This follows from the result that the activation energy of tantalum diffusion is less than or equal to the Q for self-diffusion.

[1]D. Lazarus, Phys. Rev. **93**, 973 (1954).
[2]A. D. Le Claire, Philos. Mag. **7**, 141 (1962).
[3]A. D. Le Claire, Philos. Mag. **10**, 641 (1964).
[4]A. D. Le Claire, J. Nucl. Mater. **69-70**, 3 (1978).
[5]S. M. Klotsman, V. A. Gorbatchev, Ja. A. Rabovskii, V. K. Talinskii, and A. N. Timofeev, Fiz. Met. Metalloved. **44**, 214 (1977).
[6]S. M. Klotsman, Ja. A. Rabovskii, V. K. Talinskii, and A. N. Timofeev, Fiz. Met. Metalloved. **45**, 1104 (1978).
[7]A. B. Vladimirov, V. N. Kaigorodov, S. M. Klotsman, and I. Sh. Trachtenberg, Fiz. Met. Metalloved. **48**, 403 (1979).
[8]A. Animalu, *Quantum Theory of Crystalline Solids* (MIR, Moscow, 1981).
[9]V. O. Jessin, V. G. Manakov, R. Sh. Nasirov, and D. M. Tagirova, Fiz. Met. Metalloved. **46**, 8 (1978).
[10]R. E. Pawel and T. S. Lundy, J. Electrochem. Soc. **115**, 233 (1968).
[11]N. K. Arkhipova and S. M. Klotsman, Fiz. Met. Metalloved. **46**, 796 (1978).
[12]N. K. Arkhipova, S. M. Klotsman, Ja. A. Rabovskii, and A. N. Timofeev, Fiz. Met. Metalloved. **43**, 779 (1977).
[13]N. K. Arkhipova, L. M. Veretennikov, S. M. Klotsman, G. N. Tatarinova, and A. N. Timofeev, Fiz. Met. Metalloved. **53**, 104 (1982).
[14]R. E. Pavel, T. S. Lundy, Acta Metall. **17**, 979 (1969).
[15]J. N. Mundy, S. J. Rothman, N. Q. Lam, L. J. Nowicki, and

H. A. Hoff, Phys. Rev. B **18**, 6566 (1978).
[16]J. N. Mundy, D. W. Tse, and W. D. McFall, Phys. Rev. B **13**, 2349 (1976).
[17]J. N. Mundy, H. A. Hoff, J. Pelleg, S. J. Rothman, L. J. Nowicki, and F. A. Schmidt, Phys. Rev. B **24**, 658 (1981).
[18]K. Maier, H. Mehrer, G. Rein, Z. Metallkund. **70**, 271 (1979).
[19]E. Zinner, Scanning **3**, 57 (1980).
[20]V. Naundorf and M. P. Macht, Nucl. Instrum. Methods **168**, 405 (1980).
[21]S. M. Klotsman, Fiz. Met. Metalloved. **55**, 1 (1983).
[22]Ch. Kittel, *Introduction to Solid State Physics* (Nauka, Moscow, 1978).
[23]K. Umeda and S. Kobajashi, J. Phys. Soc. Jpn. **13**, 148 (1958).
[24]C. A. Mackliet, Phys. Rev. **109**, 1964 (1958).
[25]G. Barreau, G. Brunel, and G. Cizeron, C. R. Acad. Sci. **C272**, 618 (1971).
[26]J. G. Mullen, Phys. Rev. **121**, 1649 (1961).
[27]A. Ikushima, J. Phys. Soc. Jpn. **14**, 1636 (1959).
[28]R. L. Fogelson, Ja. L. Ugay, and A. V. Pokoev, Fiz. Met. Metalloved. **33**, 1102 (1972).
[29]N. L. Peterson, Phys. Rev. **132**, 2471 (1963).
[30]R. L. Fogelson, Ja. L. Ugay, and I. A. Akimova, Fiz. Met. Metalloved. **39**, 447 (1975).
[31]A. B. Vladimirov, V. N. Kaigorodov, S. M. Klotsman, and I. Sh. Trachtenberg, Fiz. Met. Metalloved. **46**, 1232 (1978).